JOINT EUROPEAN TORUS JET

JET–P(87)39

S.A. Gohen, J. Ehrenberg, T.T.C. Jones, A. Gondhalekar, M. Bures, P. Coad,
L. de Kock, K. Erents, P. Barbour, P.D. Morgan, J. O'Rourke, J.A. Tagle,
M. Watkins and The JET Team

Particle Balance and Wall Pumping in Tokamaks

Particle Balance and Wall Pumping in Tokamaks

S.A. Gohen[1], J. Ehrenberg, T.T.C. Jones, A. Gondhalekar, M. Bures, P. Coad, L. de Kock, K. Erents, P. Barbour, P.D. Morgan, J. O'Rourke, J.A. Tagle, M. Watkins and The JET Team

JET-Joint Undertaking, Culham Science Centre, OX14 3DB, Abingdon, UK

[1]Plasma Physics Laboratory, Princeton University, Princeton NJ, 08544, USA

Preprint of Paper to be submitted for publication in
Plasma Physics and Controlled Fusion

JET P(87) 39

PARTICLE BALANCE AND WALL PUMPING IN TOKAMAKS

S.A. Cohen*, J. Ehrenberg, T.T.C. Jones, A. Gondhalekar, M. Bures,
P. Coad, L. de Kock, K. Erents, P. Harbour, P.D. Morgan, J. O'Rourke,
J.A. Tagle, M. Watkins, and the JET Team

JET Joint Undertaking, Abingdon, Oxfordshire, OX14 3EA, England
*Plasma Physics Laboratory, Princeton University, Princeton NJ, 08544, USA

ABSTRACT

The properties of carbon, with respect to its ability to absorb and release hydrogen, are reviewed and applied to the interpretation of density behaviour in Ohmic-, NBI- and ICRF-heated tokamak discharges. Based on the experimental observations, improvement of H-mode parameters in JET due to reduced hydrogen re-emission from the walls is predicted with a numerical model. The particle removal rates required for Q=1 in JET are estimated.

KEYWORDS

Tokamaks; hydrogen; carbon; fuelling; wall pumping; particle confinement; auxiliary heating.

1. INTRODUCTION

Hydrogen gas introduced into tokamak discharges will be deposited into the plasma and the material structures surrounding it. Both act as temporary reservoirs. Hydrogen may leave one reservoir by stimulated or spontaneous processes and then enter the other. The detailed hydrogen density profiles in each reservoir are determined by coupled transport equations. Thus the global particle confinement times in the materials and in the plasma affect the total particle content in each.

The term 'particle balance' refers to the relative and absolute amounts of hydrogen in the two reservoirs. 'Wall pumping' is the act in which the materials (limiters and walls) absorb hydrogen from the plasma.

Fuelling methods, plasma transport coefficients, and hydrogen recycling will control the plasma density and its profile. Their importance is illustrated by the following examples: any fuelling technique requires removal of hydrogen from the edge plasma to avoid exceeding the density limit; the record ion temperatures achieved in neutral-beam heated PLT (Eubank and co-workers, 1979) and TFTR (Hawryluk and co-workers, 1987) required gettering or wall conditioning to obtain the lowest initial density of the target plasma; the Alcator-C record $n\tau$ (Greenwald and co-workers, 1984) required pellet fuelling; the H-mode requires control of hydrogen recycling (Wagner, Keilhacker, and co-workers 1984); and the ratio of D to T and the impurity content (including helium ash) in D-T burning devices will strongly affect the Q attainable. For reasons of safety, these latter devices must also have accurate accountability and control of their tritium inventories.

Density control was first achieved by a series of pragmatically developed techniques, specifically wall and limiter conditioning by tokamak discharges. Then coatings with passive or getter films were tried and other wall-conditioning plasma processes tested (Cohen, 1984). Further methods for removing hydrogen from the plasma edge developed simultaneously and include various pump limiter (Mioduszewski, 1984) and divertor (Wagner and Lackner, 1984) configurations. Recently pumping by carbon walls (de Kock and co-workers, 1987) has gained attention.

The importance of density profiles in this and the next generation of tokamaks (e.g. Rebut and Lallia, 1987) demands scrutiny of the above-listed measures and additionally of the control of fuelling and of plasma transport coefficients. We focus on the newest phenomenon, wall pumping.

Reviews already exist for wall conditioning, pump limiters, divertors, and pellet fuelling. And success in modifying the particle transport in a favourable way may be as elusive as similar efforts to improve the plasma's thermal insulation.

In this paper we first review material properties which establish the boundary conditions for the plasma. Carbon properties are chosen as being representative because many structures in present tokamaks are manufactured from graphite, and because carbonaceous layers are known to form on the walls as a result of plasma operation (Cohen and co-workers, 1978). Measurements of the amount of hydrogen left in the tokamaks walls and limiters are then presented. The next section notes the importance of wall temperature to density control and also speculates on the mechanisms responsible for wall conditioning by low-current helium discharges (Dylla and co-workers, 1987). We then describe the density evolution in JET during Ohmic, ICRF and NBI operation to connect the material and edge plasma properties to overall tokamak behaviour. The final section is on future work. It lists the physics studies of material properties needed to elucidate the present tokamak results. This is followed by an evaluation of the density control and particle removal rate required to achieve Q=1 in JET, and the proposition that improved plasma parameters in H-modes may be attained by reducing hydrogen re-emission from the walls.

2. CARBON PROPERTIES

Pure solid carbon exists in three basic forms: diamond, graphite and amorphous. Carbon in tokamaks contains a mixture of these, but is also impure (containing hydrogen and heavier atoms), and porous. Most carbon properties were obtained in laboratory studies of pure samples, unexposed to tokamak plasmas; some data on exposed carbon samples are available. An accurate model of carbon's role in density control requires that all properties be measured for plasma-irradiated carbon.

A most important property is erosion by sputtering. For room temperature graphite the sputtering yield Y below ~ 500 eV is approximately independent of the energy E of the impacting hydrogen (Roth, 1987), in contrast to most materials. This is attributed to chemical effects such as formation of volatile hydrocarbons. Above 500eV the sputtering yield falls with increasing energy. (At 500°C the yield increases a factor of 2 as the energy increases from 20 eV to 300 eV and then falls for $E \gtrsim 500$ eV.) For monoenergetic deuterium impacting graphite, the maximum sputtering yield is 0.03 at room temperature and 0.2 at 550°C, again due to chemical synergy. The physical sputtering yield changes little with impurity content of the carbon while the chemical yield decreases (Behrisch, 1987).

For a fixed power loss from the plasma through the conduction channel, the maximum carbon production rate, ΓY, by hydrogen impact (fig.1) occurs at a low energy, below 20 eV. For carbon ions impacting carbon limiters, the maximum rate, again for fixed power loss, is at about 150 eV, where the physical sputtering yield is proportional to energy (Lackner and co-workers, 1984). Therefore tokamak operation at edge temperatures above ~ 50 eV should result in lower carbon influx by ion sputtering.

Direct and immediate kinematic reflection will occur for a fraction of hydrogen atoms which impact solid carbon. The measured reflection coefficient (for normal incidence deuterium on graphite) is also shown in fig. 1 (Behrisch and Eckstein, 1984; Chen, Scherzer, and Eckstein, 1984). No data exists below 300 eV where the reflection coefficient is ~ 0.3. Calculations indicate that the reflection continues to increase down to about 10 eV (Eckstein and Heifetz, 1987). These data too point to the benefits of a high edge temperature, in this case to reduce reflection of the impacting

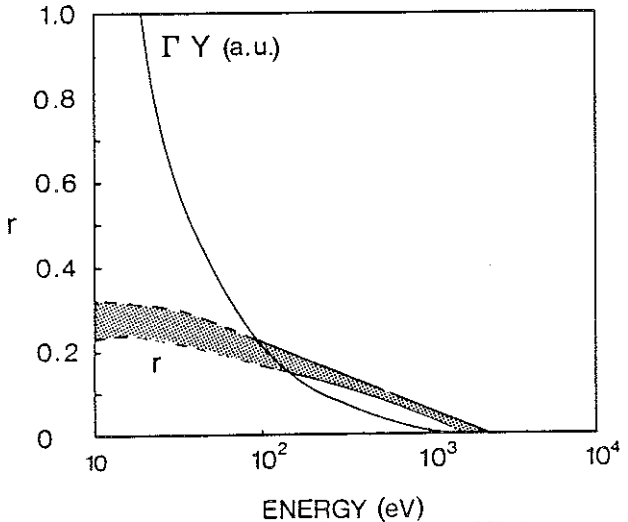

Fig.1 Particle reflection coefficient, r, and impurity generation rate, ΓY, at fixed power loss for normal incidence deuterium impact on room temperature graphite.

hydrogen by the graphite. No change in reflection coefficient occurs for hydrogen-loaded carbon surfaces while an increase in reflection occurs for surface contamination by heavy impurities such as iron.

Particles impacting the carbon lattice create damage by breaking bonds and displacing carbon atoms. The damage acts as trapping sites of about 4.6 eV depth for hydrogen (Wilson and Hsu, 1987). At room temperature the density of the hydrogen in the traps can reach 40% of the bulk carbon number density. Intrinsic traps, ~ 4 eV deep, occur in unirradiated bulk graphite at a level of about 20 ppm. The penetration of energetic hydrogen ions into bulk carbon (Andersen and Ziegler, 1977) is about 2×10^{-11} m/eV in the energy range 20 eV < E < 20 keV. In beam-solid experiments, the beam is first strongly absorbed by the graphite target. But the amount of retained hydrogen increases towards a saturation value (Staudenmaier and co-workers, 1979) approximately as $[1-\exp(-F/N_s)]$, where N_s is the energy-dependent saturation value ($\sim 2 \times 10^{21}$ $E^{0.8}$ (keV) m^{-2}) and F the fluence. The saturation level decreases with increasing temperature from 40% at temperatures below 300°C to about 5% at 700°C.

The impact of any type of energetic ion or neutral onto hydrogen-loaded carbon can result in release of the hydrogen from the traps. The initial cross-section (Wampler and Doyle, 1987) for such release is shown in fig. 2, where the abscissa is the nuclear energy loss rate from the impacting particle to the carbon lattice. From the straight-line model we estimate that for a 0.5 keV proton the cross-section is about 5×10^{-21} m^2 (Andersen and Ziegler, 1977). As the energy of the impacting proton decreases, it eventually becomes ineffective in desorbing trapped gas because of its reduced range and reduced available energy. Once released from the traps, hydrogen is observed to leave the lattice and enter the gas phase as molecules (Scherzer, Borgesen, and Möller, 1987). In beam-solid experiments when the retained hydrogen approaches the saturation value, further bombardment results in 100% re-emission, initially with the trapped particles leaving the graphite and the bombarding particles replacing them in the traps. If a room temperature graphite sample is saturated by bombardment with keV hydrogen and then heated to ~ 600°C during continued bombardment, initially the re-emission will exceed 100%. Except for this case, no ion-induced desorption experiments have shown re-emission greater than unity. Of course, room temperature unconditioned materials, e.g., hydrocarbon-contaminated, will show desorption yields greater than unity, but this has not been observed for hot, T > 300°C, conditioned graphite. Desorption by light particles, electrons or photons, is expected to be less important. However, this needs direct verification in an intense radiation environment typical of tokamaks.

Once beam irradiation has ceased, a hydrogen-implanted carbon sample has its hydrogen density distribution determined by its temperature-dependent diffusivity and the boundary conditions, including the internal porosity. This is about 1 m^2/gm for unirradiated POCO graphite (Causey,

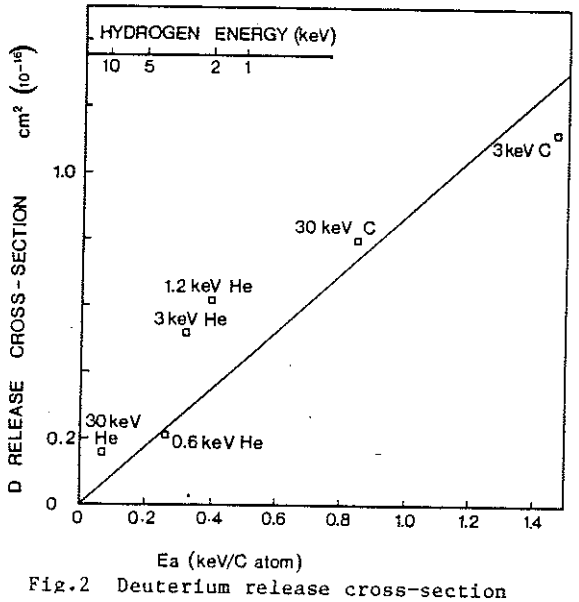

Fig.2 Deuterium release cross-section versus energy into atomic collisions for various particles impacting deuterium-saturated room temperature graphite.

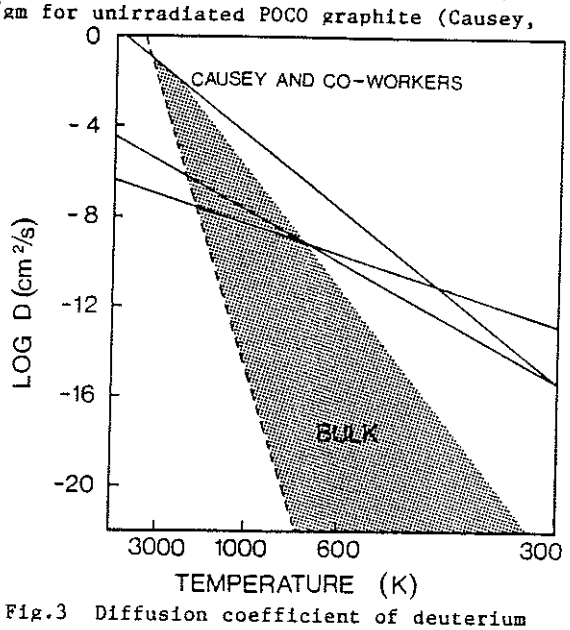

Fig.3 Diffusion coefficient of deuterium saturated room temperature graphite. The solid lines are estimates of surface diffusivity.

Baskes, and Wilson, 1986). Microscopic examination of graphite exposed to hydrogen plasmas shows that an open porous structure develops to depths in excess of 10 microns (Goebel and co-workers, 1987). The structure is sponge-like, with typical voids of 1-10 microns diameter and walls less than 1 micron in thickness. Based on these micrographs, a crude lower limit of the porosity is 20 m^2 of microscopic area per m^2 of macroscopic surface. Nakamura and co-workers (1986) measured surface roughness factors as high as 100 for graphite irradiated by 1.5×10^{18} cm^{-2} 3 keV D.

Causey, Baskes and Wilson (1986) categorize two main types of hydrogen diffusion in unirradiated graphite, fig.3. Diffusion through the bulk becomes important for temperatures above ~ 1000 K. The activation energy is between 2 and 5 eV. This process is poorly understood, so the grey-hatched area in fig.3 should only be considered as an estimate. The other diffusion process, characterized by traps of depth 0.4 - 0.9 eV (and possibly as low as 0.15 eV (LaMarche and co-workers, 1986)), is thought to occur on the surface of graphite microcrystallites. This can affect the hydrogen density distribution at temperatures as low as 100°C. It is expected that impurities, hydrogen content, porosity, and radiation damage will change the diffusion and recombination of hydrogen in carbon (Amemiya, 1987).

Thermally activated release of implanted hydrogen shows (Nakamura and co-workers, 1987) that at fluences above 10^{16} cm^{-2} molecular hydrogen is thermally released at temperatures as low as 100°C. The peak release rate is at about T ~ 600°C, in agreement with Philipps and co-workers (1987).

The final process relevant to wall pumping is the build-up of hydrocarbon films on cool surfaces near a warm plasma-irradiated graphite sample (Hsu and Causey, 1987). This phenomenon, termed 'co-deposition', is ostensibly due to chemical sputtering. It is a non-saturable mechanism for pumping hydrogen. Diffusion of hydrogen into bulk graphite would also effectively show no saturation because of the huge capacity of the bulk.

3. HYDROGEN IN TOKAMAK WALLS

The aforementioned phenomena show several ways by which hydrogen may be incorporated within the carbonaceous structures found in tokamaks. There are two methods to measure the hydrogen left behind in the walls and limiters of a tokamak after a discharge. The first is to measure directly the hydrogen in the walls. Using ion-beam techniques capable of probing to 1 micron depth, several hundred such measurements on JET components and samples of wall and limiter areas (Behrisch and co-workers, 1987; Bergsåker and co-workers, 1987) were performed. Note that hydrogen which has diffused further into the bulk remains undetected by this analysis method. In the pre-ICRF, pre-NBI 1985 operating period, the retained hydrogen isotopes concentrations reached levels as great as 2×10^{22} m^{-2}, corresponding to carbon layers saturated to depths of 0.5 microns. This depth rules out direct implantation of plasma ions as the cause of the high concentrations. (Energies of 70 keV are required to penetrate 0.5 micron.) Averaging over the entire interior surface area of JET, the total amount of retained deuterium within the first micron was about 10^{24} atoms. Co-deposition during tokamak discharges is a possible cause. But our model of co-deposition during discharge steady state fails by a factor of 10 to reproduce such high hydrogen deposition rates. We believe a more likely cause was the extensive use of glow discharge carbonization during this period. In support of this view are results from the 1986 campaign, which included ICRF and NBI and little carbonization. Ion beam analysis showed that the total retained amount of deuterium was about 5 times less than in 1985 (Behrisch, 1987) and corresponded to about 1% of the gas fuelled during the 1986 period. (Hydrogen was not measured but was expected to be small because few discharges were fuelled with hydrogen.) The concentration was highest on structures near the plasma edge, but not those subject to the most intense particle and heat flows. In 1985 deuterium was found approximately uniformly around the walls; in 1986 it was concentrated on the inner wall, in agreement with the more extensive use then of the carbon-tiled inner wall as a limiter.

The second method is to measure the gas pumped out of the tokamak after a discharge and compare it with that puffed in during the discharge. Fig.4 shows such a measurement performed in JT-60 (Nakamura and co-workers, 1986). Immediately after the discharge most of the gas was trapped in the walls. Several seconds after the discharge the pressure rose to a peak and then decayed, in proportion to 1/t. For Ohmic discharges, the JT-60 team found the pumped deuterium ranged from 40% to 80% of that introduced in the pulsed gas feed. Assuming a continued 1/t re-emission, it would take about 10^4 s (for the 80% case) to 10^9 s (for the 40% case) to re-emit all the deuterium. Experiments on ASDEX, a machine with no carbon components, showed about 90% of the

injected gas pumped away in the 15 minutes after each discharge (Wang, Poschenrieder, and Venus, 1986). Measurements on TFTR (a machine with tens of square meters of graphite components and cool walls) after helium conditioning show the pumped deuterium to be initially 12% of that introduced into a discharge (Dylla and co-workers, 1987). After about 12 shots the walls were de-conditioned, but the pumped amount increased to the asymptotic value of only 25%. This has been taken as evidence of co-deposition, which may occur during discharge start-up, steady state, or termination.

The pressure after a discharge in JET is also shown in fig.4, along with the pressure with a gas puff only (no plasma). From these we can get a measure of the characteristic time during which hydrogen leaves the vessel walls after being implanted by the plasma. This is seen to be $\gtrsim$50 s.

For the upcoming tritium experiments ways to remove this retained hydrogen are being developed which rely on thermal, erosion, replacement, and desorption mechanisms described in section 2.

4. WALL CONDITIONING

Numerous reviews have been written on impurity control by wall conditioning methods (Dylla, 1980; Cohen, 1984), including the new technique of carbonization (Winter, 1987a). Density control can also be effected by wall conditioning. Two new results are noted here, the first pertains to wall temperature, the second to desorption.

Figure 5 shows the time evolution of two series of discharges in TEXTOR, with each series interrupted by 20 minutes of rf glow discharge cleaning (rfgdc) in pure deuterium (Winter, 1987b). (One month prior to these experiments, TEXTOR had been extensively carbonized.) In the first series, a), the wall temperature was 150°C. With the same gas feed into each discharge, the post-rfgdc discharges (22821-26) displayed a higher density, indicating an increase in the global recycling coefficient, presumably due to wall loading with deuterium. In contrast, the second series of discharges, with the wall temperature at 350°C, showed a reduction in the density of those discharges after the rfgdc (23346-52), clearly indicating a decrease of deuterium in the carbonized film near its surface. The conclusion is that a carbon wall temperature in excess of ~ 300°C will result in appreciable wall pumping. Presumably, the lattice stores the hydrogen for a few seconds during a discharge; then thermally activated diffusion and desorption empty the near-surface carbon lattice between discharges.

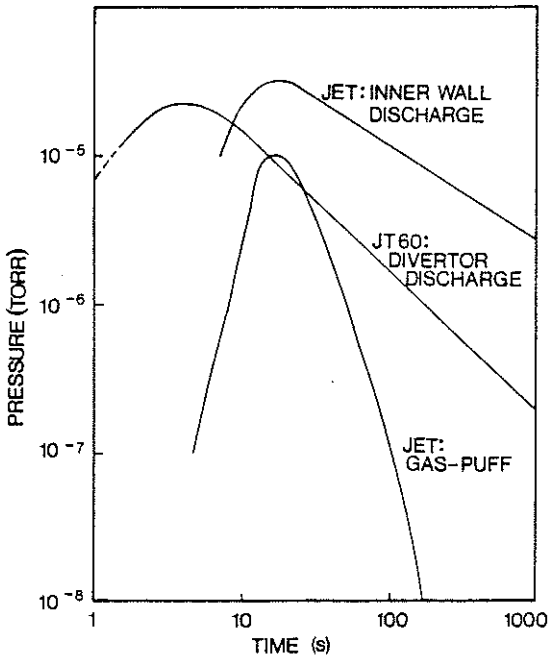

Fig.4 Pressure versus time after Ohmic discharges in JT-60 and JET. Also shown is JET data for a gas puff only.

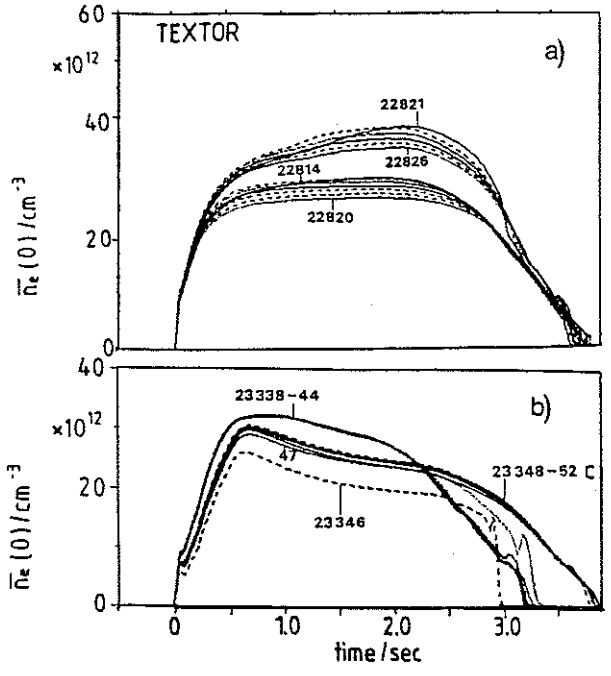

Fig.5 Plasma density versus time for two sets of discharges in TEXTOR. The wall temperature was 150°C in a) and 350°C in b).

The success of low current (I_p < 1 MA) helium conditioning pulses in producing low density target plasmas has been attributed to helium and carbon ion-induced desorption (IID) of the hydrogen occupying the deep damaged-induced traps (Dylla and co-workers, 1987). Continuing the IID line-of-reasoning we first note that the scrape-off distance is longer at lower plasma currents (Tagle and co-workers, 1987). It is important that the helium ions reach (scour) more distant surfaces which are exposed to charge-exchange neutrals during hydrogen discharges. Furthermore, an optimal energy exists where the impacting ions penetrate far enough into the carbon and still have a high enough desorption cross-section. This energy is about 500 eV for helium impact, requiring an edge electron temperature of ~ 65 eV. Tagle and co-workers (1987) have shown that this occurs in JET only at low plasma currents and at a density of about 10^{19} m^{-3} for helium. A subtle reason for the superiority of helium over hydrogen (or deuterium) in the conditioning discharges is that the ion density in the edge in helium discharges is higher than in hydrogen discharges. (The most likely cause for this is the lack of Franck-Condon events for helium keeps the ionization source nearer the plasma edge.) Hence the flux onto surfaces is higher. And obviously, hydrogen cleaning is less effective than helium because it reloads the lattice.

Another reason is the delicate balance between ion induced desorption and thermal diffusion. Ehrenberg (1987) and others (Causey, Baskes, and Wilson, 1986; LaMarche and co-workers, 1986) have shown that there is a large reservoir of hydrogen within the bulk of the carbon. When the plasma current is high, the power into the plasma increases, increasing the thermal load on the limiter (McCracken, 1987). Then hydrogen desorbed from the near-surface region may be replenished by hydrogen diffusing out of the bulk. Another contributing factor to the benefits of low current operation for wall conditioning is the better confinement of the desorbed hydrogen in the lower density plasma causing less prompt reimplantation.

5. DENSITY BEHAVIOUR IN JET

Efforts have been made on JET to compare the plasma density evolution with numerical models (Ehrenberg and co-workers, 1987; Jones and co-workers, 1987; Bures and co-workers, 1987) based on the previously described properties of carbon and of the plasma. Concerning the latter, experiments (Cheetham and co-workers, 1986; Hubbard, Ward, and Stringer, 1986; Gondhalekar and co-workers, 1987; Cohen and co-workers, 1987; Stangeby and co-workers, 1987) under a variety of JET conditions have shown nearly the same plasma particle transport coefficients. These are a diffusivity of 1 m^2/s at the edge and 0.3 m^2/s on axis, and an inward convection proportional to minor radius equal to ~ 0.1 m/s at the edge. The equations describing density evolution are the local flux and conservation equations. Insight may be gained by recasting these equations into the global form of the two reservoir model.

$$\dot{N}_p = -(1-r_w)\frac{N_p}{\tau_p} + (1-r_p)\frac{N_w}{\tau_w} + \phi \qquad (1)$$

where N_p = total hydrogen content of the plasma,
τ_p = global particle confinement time in the plasma,
r_w = kinematic reflection coefficient of the wall,
N_w = total hydrogen content in the walls,
τ_w = global particle confinement time in the walls,
r_p = reflection coefficient of the plasma, and
ϕ = the fuelling source.

The definition of a residence time in (or on) the walls clarifies its role as a reservoir. In steady-state, i.e., no fuelling and 100% recycling, the particles will divide themselves between the two reservoirs proportional to their effective confinement times in each, where the effective confinement time includes the reflection coefficient factors.

In the actual numerical evaluations of the flux equations, separate carbon properties are used for the inner wall, wall, and limiters. The diffusion equation of hydrogen in carbon is solved, including a source term dependent on impact energy, and boundary conditions appropriate to first- or second-order release from the surface. Impurities are taken into account using the measured Z_{eff} to modify N_p. The flux out of the walls back into the plasma consists of three

terms, two prompt (the kinematically reflected and the desorbed) and one slow (the diffusing/recombining) part. The two prompt terms are proportional to N_p/τ_p, the first term on the RHS of eqn.(1). The essence of the slow part is embodied in the global particle confinement time in the wall, τ_w, defined in the same way that the global plasma particle confinement time is defined, thus $\Gamma_w A_w = N_w/\tau_w$, where Γ_w is the flux out of the wall into the plasma and A_w the wall area. Particles entering the plasma may be 'reflected' (Voss, 1980) by charge exchange or Franck-Condon processes, summarized by the probability factor r_p, which is estimated to be 0.5.

The flux equation in the entire plasma may be solved in each interval of time using transport coefficients and fuelling profiles obtained from plasma and atomic physics codes, or the plasma particle confinement time may be treated as an explicit function of plasma parameters. From H-α measurements we find for ohmically heated deuterium plasmas

$$\tau_p \simeq 2 \times 10^3 \text{ R(cm) a(cm)}^2/\text{n(cm}^{-3})^{0.8} \text{ sec.} \qquad (2)$$

The density dependence agrees with that predicted by Engelhardt and Feneberg (1978) for gas-fuelled discharges and with that noted by Stangeby (1987). In these Ohmic discharges there is no strong dependence on B_T or I_p. The dependence on the mass of the background gas is relatively weakly documented - both helium and hydrogen having somewhat shorter confinement then deuterium. During auxiliary heating, the particle confinement time decreases a factor of 2 in L-mode discharges and increases about a factor of 2 in H-mode discharges. Fuelling on axis, as by NBI, only alters the particle confinement time in a transient manner because edge recycling occurs at a high rate compared to the central fuelling rate.

For diffusion-dominated release of hydrogen from the wall, the particle confinement time in the wall may be estimated from the diffusivity and range data in section 2. For the surface diffusivity, τ_w is about 1 s at 200°C. But the rate will depend strongly on temperature, changing a factor of 10 as the temperature changes 100°C. We again point out that the diffusivity through carbon in tokamaks may be quite different from that in unirradiated samples. One might suggest that the best measure of τ_w is that derived from the release of gas after a discharge. But the > 50 s value of τ_w is inconsistent with the fuelling efficiency and particle balance to be described in the next section. We conclude that the processes occurring during discharge termination, the so-called 'soft landing', are different than during the steady state.

5.1 Ohmic Heating

To study the role of material and plasma properties in determining the density in ohmic plasmas discharges of various initial densities were formed on the outer carbon limiters (macroscopic area ~ 1 m^2) then moved to the carbon-tiled inner wall (macroscopic area ~ 20 m^2) (Ehrenberg and co-workers, 1987). During each discharge the plasma was shifted back and forth between the limiters and inner wall twice. The movements took 400 ms each, and the residence time on each surface was 4 seconds between moves. The time evolution of the gas feed, N_D, and H-α emission from the limiters and the inner walls is shown in fig.6 for five discharges in the series. Only in the first discharge (11019) was the plasma not shifted. A deuterium pre-fill was introduced into the vessel about 0.5 s before each discharge. Note that in discharges 11020, 11022 and 11023 the subsequent dosing gas feed was shut off at 4 s, while in 11024 the dosing feed was never turned on. In spite of no gas feed during the time 0 to 4 s, the density in 11024 still rose, indicating a continuous fuelling of that discharge for at least those first four seconds. The source of the fuelling is predominantly the release of hydrogen from the walls and limiters.

The number of electrons in the plasma of 11024 represents at most (at t = 4 s) 50% of those introduced with the gas feed. The fuelling efficiency decreased with increasing density, which Ehrenberg and co-workers show is indicative of diffusion-limited (or another first-order process) release of the hydrogen from the walls. This considerably eases solution of eqn.(1) by eliminating a free parameter, the recombination coefficient.

When the plasma is moved to the inner wall the density drops. The density asymptotically approaches a lower level, consistent with a new balance between wall pumping and outgassing or between τ_p and τ_w. The maximum decay rate measured was 2×10^{21}/s in this experiment. On repositioning the plasma on the outer limiter the density rises, approximately back to its value at 5 s. The initial rate of rise is typically 6×10^{20}/s.

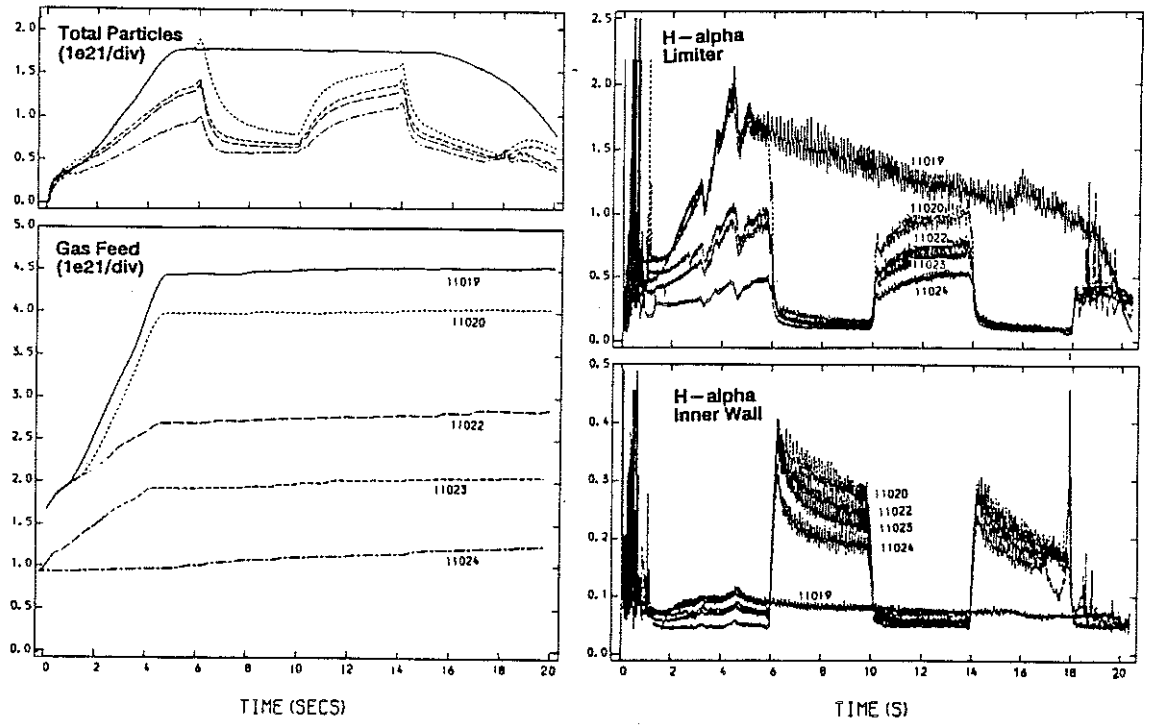

Fig.6 Time evolution of 4 parameters for 5 discharges: 11019, 11020, 11022, 11023 and 11024. 11019 was always positioned on the outer limiters; the others were started on the outer limiter, moved to the inner wall at 6 s, moved back to the limiter at 10 s, back to the inner wall at 14 s, and back to the limiter at 18 s.

The pumping ability of the inner wall showed no saturation after 10 such discharges in the sequence. Had bombardment-induced deep traps been responsible for the pumping, these would have saturated in 2 seconds, based on the particle fluxes, or in 2 discharges, based on the gas fuelled. These estimates allow for an edge plasma temperature of up to 200 eV, the entire inner wall being completely free of hydrogen, and a wall temperature below 300°C. We conclude that this mechanism is unimportant in this pumping experiment.

The continuous outgassing of the walls is demonstrated by the non-zero value to the H-α radiation from the inner and upper wall during the time the plasma resides on the limiter. A quantitative evaluation of the electron source rate from the H-α brightness gives 6×10^{20}/s. The initial source for this outgassing is the discharge initiation which loads the walls with 50-70% of the prefill gas. As this source empties it is replaced by hydrogen implanted by charge exchange. Note that a fuelling efficiency of 50% implies $\tau_p \sim \tau_w \sim 0.5$ s, indicating the inapplicability to analysis of the steady state of τ_w determined from post-discharge outgassing.

The initial rapid rise of density when the plasma is repositioned on the outer limiter is mainly the result of wall outgassing and the inability of the outer limiters to absorb (more) hydrogen. Ion-induced desorption of hydrogen from the near-surface of the limiter (replenished from deep within by thermally activated diffusion) may contribute up to ~ 20% in the initially rapid rise, as estimated from H-α. We have shown by probe measurements that when the plasma is on the inner wall very few ions impact the outer limiters. Hence the density rise is not due to release of the hydrogen ions implanted in the limiters when the discharge was on the inner wall. The salient point is that the density rise is most closely connected to the amount of gas injected by the dosing and prefill for that discharge only.

Why the inner wall configuration pumps so well compared to the limiter is still a matter of speculation. The H-α signals indicate that a significant (> 30%) part of the 're-fuelling' comes from the top/bottom walls. It has been suggested that different diffusion coefficients exist because of different materials (possibly temperatures) at the walls and limiters. Ehrenberg achieves excellent agreement between the experiment and numerical integration of eqn.(1) using

diffusion coefficients of order $10^{-11,-12}$ cm^2/s and a finite thickness to the material of about 50 nm. The layer thickness L is related to the diffusion coefficient D, such that $\tau_w \sim L/D$. The layer thickness may be related to structure Goebel and co-workers observe. The global particle confinement in the wall calculated by Ehrenberg is about 1.25 s, and is amplified by the recycling and reflection processes near the plasma edge to about 4 s. The confinement time is shorter in the warmer limiter by a factor of 10. The kinematic reflection coefficient in this model is 0.3.

Another model depends on the different carbon areas. This requires a porosity of 15 m^2/m^2 to sorb 5×10^{21} atoms in each discharge. Using the entire area of the inner wall, either surface adsorption (to a maximum areal density of 2×10^{15} cm^{-2}) or supersaturation of the carbon lattice (to 10% above the 0.4 value described in section 2) would require a surface roughness factor in excess of 15, which is expected. But neither a supersaturated bulk or surface layers of such high areal density for deuterium on carbon have been reported. And the correct residence time for deuterium in or on the carbon is required.

Also different edge plasma parameters may occur because of its different configuration. A two-fold drop in τ_p when the plasma is moved onto the inner wall would explain the density behaviour. We do not have sufficiently accurate H-α data to rule out changes in τ_p.

Thus, we know wall outgassing is important. Though good simulations of the density behaviour in Ohmic discharges have been achieved we must conclude that there is not yet data to select between the various plausible mechanisms for temporary hydrogen storage by carbon. However, an important parameter, τ_w, has been measured and future experiments should clarify the relevant processes.

5.2 Neutral-Beam Injection

The density rises during NBI by an amount that depends on wall conditions and plasma configuration (Jones and co-workers, 1987). In fig.7 are shown three cases. For unconditioned inner wall or x-point operation the density rises at an initial rate that is about twice the beam fuelling rate. The thermal part of the edge plasma (Erents, Tagle and McCracken 1987) does not respond as quickly as the density rise, indicating that it is not responsible for desorbing atoms. Heating the walls and limiters is estimated to be too slow to account for the density rise. And the loss of fast ions is not expected to result in a great desorption yield both because of the small losses and the small cross-section, e.g. fig.3. One possible cause is neutral-impact desorption by the charge exchange flux resulting from thermal plasma ions charge exchanging with the neutral beam. As indicated in section 2, greater than unity desorption yields require hydrocarbon (not carbon) films. After conditioning with helium, the best inner wall discharges show an initial rate of density rise equal to the beam current.

Jones has modelled the density behaviour in these discharges. He assumes a global model of the solid, using τ_w instead of a separate diffusion term. The best fit to his data results with $\tau_w = 1$ s, in good agreement with the Ohmic JET models. The asymptotic density rise in the unconditioned inner wall discharges is found from his model to be the beam-fuelling rate times $\tau_p/(\tau_p + \tau_w(1-r_w)/(1-r_p))$.

After termination of NBI into limiter plasmas, the density in a discharge remains above its preinjection value, as in most gas-and pellet-fuelled discharges (Cohen and co-workers, 1987). This is explained by the ratio of confinement times in the Jones model equations. NBI with conditioned walls results in the post-injection density reverting to its preinjection value because of the availability of deep traps to the 'hard' charge exchange neutral spectrum during NBI.

During the H-mode, the plasma particle confinement time doubles and the edge temperature increases above 1 keV about 5 cm inside the separatrix. The drop in H-α light at the divertor plate is then due to the decreased hydrogen ion flux, the decreased kinematic reflection coefficient at the divertor plate, and the decreased desorption cross-section. The initial density rise during the H-mode transition is at about 2.5 times the beam current. The same factors contribute to this density rise as in the case of the unconditioned inner wall, namely outgassing, ion- and neutral-induced desorption, and beam fuelling.

5.3 ICRF Heating

The application of ICRF power to tokamaks results in an instantaneous (t < 0.2 ms) change in the edge plasma (Cohen and co-workers, 1984). The scrape-off layer broadens, causing an increase in ion flux to the wall. The ions neutralize, re-enter the plasma, and cause charge exchange events. Probably the subsequent neutral flux to the walls causes desorption of hydrogen, hence the density rise. Once again a desorption mechanism must be found with greater than unity yield. The density rise during ICRF heating is less at higher currents. Then the walls are proportionally less important than the limiters as sources of gas.

In early JET operation (Cheetham and co-workers, 1986) the density rise associated with ICRF heating increased linearly with power. But continued JET operation has reduced the density rise by a factor of 3, (fig.8) with saturation evident. More recently, helium conditioning has further reduced the density rise another 30-50%. Additional decreases in density rise occur using different antenna configurations (Bures and co-workers 1987).

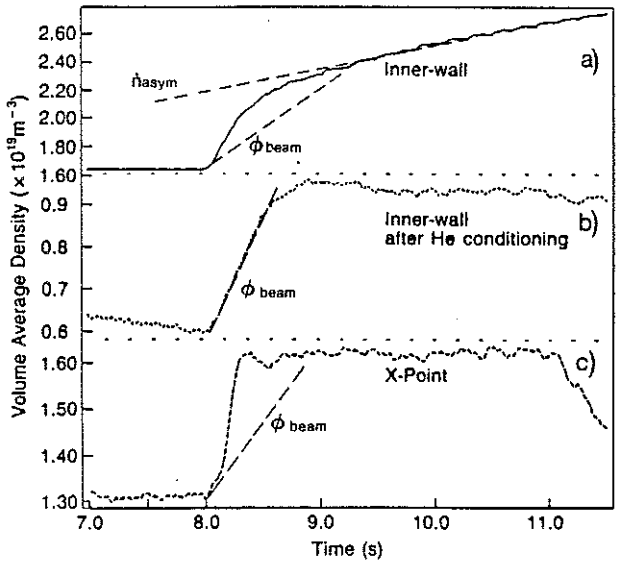

Fig.7 Density rise during NBI for three cases. Also shown is the fuelling rate, ϕ_{beam}, and the asymptotic density rise.

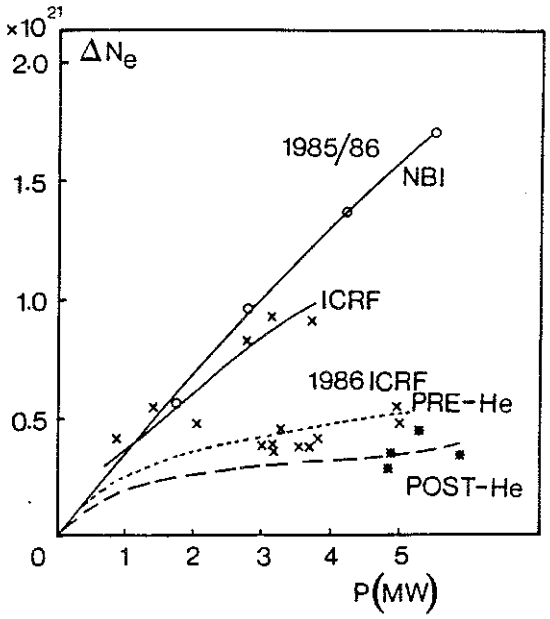

Fig.8 Density rise versus auxiliary heating power for two different operational periods, 1985/1986 and 1986. Reduced density rise was attained during 1986 both by ordinary conditioning (.....) and helium conditioning (-----).

Bures and co-workers (1987) have modelled the evolution of density during ICRF heating. They find the most important term in eqn.(1) is the desorption, which is characterized by two different time scales. Rapid desorption is due to the rapid edge modification caused by RF power absorbed in the edge plasma. A slower desorption occurs, driven by the diffusion of heat out of the core of JET. Again, there is a need to find a process involving carbon bombardment that results in the liberal (greater than unity) release of absorbed hydrogen atoms.

6. FUTURE PLANS

Certain basic materials properties of tokamak-plasma-irradiated carbon must be measured to fully understand the present results and predict future behaviour. The main questions concern hydrogen transport through the damaged and impure lattice. Does hydrogen transport occur between or across graphite planes, along free surfaces, or through stacked faults? What is the thermal activation energy for the transport? Does a supersaturated state exist? Is diffusion in the graphite lattice hindered at high hydrogen concentrations? What is the accessible porosity of irradiated graphite? Are there really only two depths to the hydrogen traps in damaged graphite? Where does recombination to molecules occur? Is desorption in tokamaks spontaneous (thermally activated) or

stimulated by particle impacts? These questions can be answered in the laboratory and must be verified on the tokamaks. In addition, a larger database must be formed of measurements of the hydrogen left in tokamak walls so that the tritium issue and desorption yields can be properly addressed. Detailed post-discharge wall outgassing studies must be made for a variety of discharges. And suggested techniques for removing tritium from the walls should be tried.

The success of low current helium discharge conditioning reopens the question of how to obtain optimum conditioning. One way is with helium glow discharges. In this manner all surfaces are bombarded, not just those nearest the edge plasma. In addition no thermal load - which might act to enhance diffusive repopulation of the depleted surface - is placed on the structures.

As previously described, wall pumping is a desirable if not an essential capability for long pulse operation. How much then is required? We can use the Q=1 case described by Bickerton and co-workers (1987) as a baseline for JET. The average density must be kept at or below 4×10^{19} m^{-3} to have a high enough temperature with the maximum available heating power, 20 MW of NBI and 20 MW of ICRF. If the fuelling were all by neutral beams and the particle confinement time were L-mode, one can readily calculate the particle losses using eqn.(2). This gives a required recycling coefficient of about 0.98, equivalent to 1.5×10^{21}/s of pumping. This has been achieved with the inner wall for a few seconds. For longer duration NBI, both the sorption and power handling capabilities of the inner wall may be stressed. With this high recycling at the edge, a broad profile will result. If a peaked density profile is required to optimize Q, then the location of the fuelling must be better controlled. Core fuelling, as with pellets, must augment the beam fuelling and the wall pumping increased to reduce the edge source. Fig.9 shows the peakedness in the density profile obtainable by altering the ratio of edge, S(a), to central, S(0), fuelling. By decreasing the recycling coefficient to 0.89 and injecting 4.5×10^{21} atoms/s in pellets, the peakedness can be increased to 3 in steady state. The total pumping now required is 6×10^{21}/s, a value never attained. However a pump limiter could be used. Dietz and co-workers, (1987) have designed for JET a pump limiter with an estimated pumping speed equivalent to a recycling coefficient of 0.9. If a higher peakedness is desired, based on our present understanding of wall pumping, pump limiters, and plasma transport, it could only be accomplished in a transient manner. In fig.10 is shown the time evolution of the peakedness and τ_p for a discharge (with standard plasma transport coefficients) heated by NBI and fuelled by pellets. Of

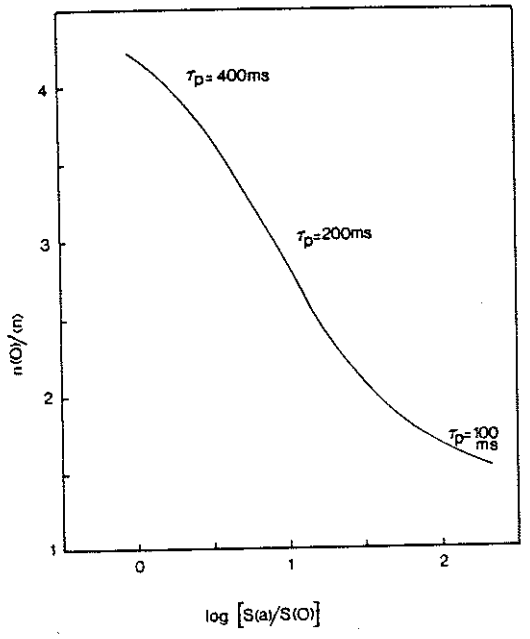

Fig.9 Density profile peakedness, n(0)/<n>, versus location of the electron source. S(a) and S(0) are respectively the electron creation rates near the limiter radius and near the plasma axis.

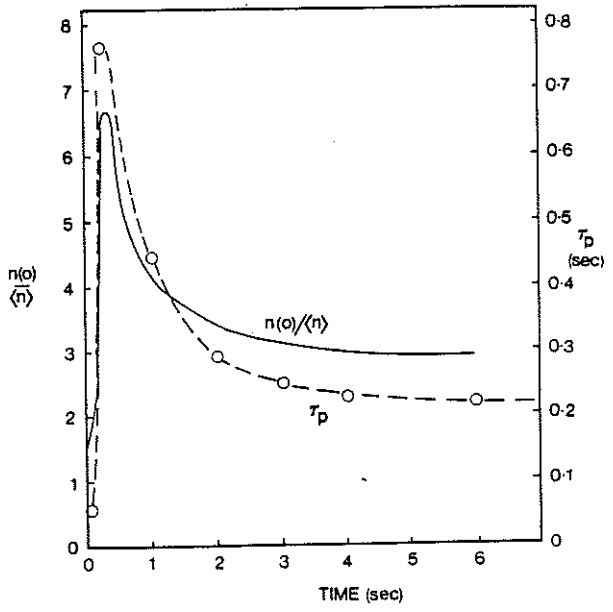

Fig.10 Computed time evolution of the density peakedness and particle confinement time for a JET discharge fuelled with a pellet containing 4×10^{21} atoms at t = 0.05 s and then continuously with 20 MW of 120 keV NBI. The recycling coefficient was set to 0.9.

course, a lowering of the particle diffusivity on the JET axis to increase τ_p there to 10 seconds would also increase the peaking for a longer duration.

The outgassing of the walls observed in JET discharges provides an unwanted and an as-yet-uncontrolled fuelling with cold gas. Better discharge initiation and wall conditioning could eliminate this in the future. What benefits would occur? We examine the effect on H-modes by the following 1 1/2-d simulation of JET discharges with auxiliary heating. Good simulations of Ohmic and L-mode phases are obtained using the critical temperature gradient model for electron energy transport (Rebut, Watkins, and Lallia, 1987). If in these calculations the edge particle transport is modified by reducing the particle diffusion coefficient to 1/4 its standard value in the vicinity of the separatrix, pedestals on the edge temperature reminiscent of the H-mode form. This ansatz of a reduced particle diffusivity is consistent with the experimental observations of reduced recycling fluxes during H-modes. If the additional gas fuelling due to outgassing, 6×10^{20}/s, is shut-off in the calculations, even higher pedestals in temperature occur (fig.11), leading to increased stored energy and higher central temperatures. We also speculate that an influx of cold gas leads to the termination of H-modes by its adverse effect on the edge temperature. Hence reduced edge fuelling by reduction of wall outgassing will result in a longer duration of the high edge temperature and the H-mode itself.

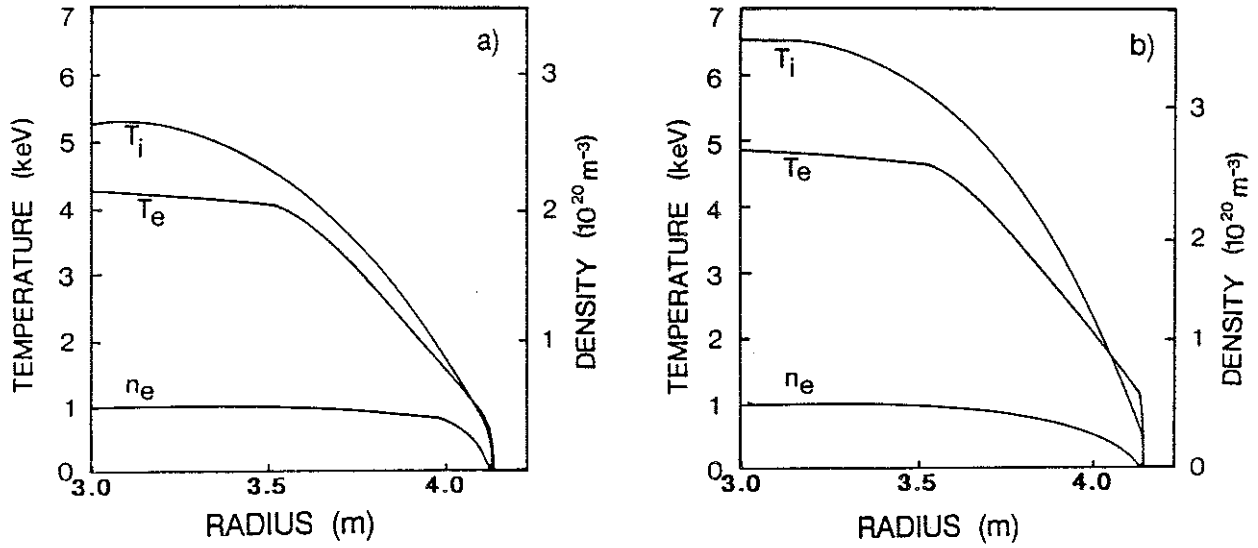

Fig.11 Calculated density and temperature profiles for two JET-like plasmas. The transport coefficients are described in the text. The wall outgassing was set to 6×10^{20}/s in a) and 0 in b). Note the higher central and edge temperatures in b) for these H-mode simulations.

ACKNOWLEDGEMENTS

We thank Dr R Behrisch and Prof P C Stangeby for their comments and Drs H F Dylla, H Kishimoto, W Poschenrieder, M Redi, B Wampler, P Wienhold, J Winter and M Yoshikawa for unpublished data.

REFERENCES

Amemiya, S. (1987). In T. Yamashina (Ed.), Characterization of Graphite as a First Wall and Evaluation of the Stability Against Plasma, Hokkaido University, Sapporo, pp.52-60.

Andersen, H.H. and J.F. Ziegler (1977). The Stopping and Ranges of Ions in Matter, Vol.3, Pergamon Press, New York.

Behrisch, R. and W. Eckstein (1984). In D.E. Post and R. Behrisch (Ed.), Physics of Plasma-Wall Interactions in Controlled Fusion, Plenum Press, New York, pp.413-438.

Behrisch, R. (1987). Private communication.

Behrisch, R., J. Ehrenberg, M. Wielunski and co-workers (1987). J. Nucl. Mater. 145-147, 732-726.

Bergsåker, H., R. Behrisch, J.P. Coad, and co-workers (1987). J. Nucl. Mater., 145-147, 727-730.

Bickerton, R.J., and the JET Team (1987). Plasma Physics & Controlled Fusion. This volume.

Bures, M., V.P. Bhatnagar, M.P. Evrard, and co-workers (1987). Proceedings 13th European Conference on Controlled Fusion and Plasma Physics, Madrid, Vol.11D, Part II. pp.722-725.

Causey, R., M.I. Baskes, and K. Wilson (1986). J. Vac. Sci. and Technol., A4, pp.1189-1192.

Cheetham, A., J.P. Christiansen, S. Corti, and co-workers (1986). Proceedings 12th European Conference on Controlled Fusion and Plasma Physics, Schliersee, Part I. pp.240-243.
Chen, C.K., B.M.U. Scherzer, and W. Eckstein (1984). Appl. Phys. A. 33, pp.265-268.
Cohen, S.A., H.F. Dylla, S. Rossnagel, and co-workers (1978). J. Nucl. Mater, 76/77, pp.459-471.
Cohen, S.A., D. Ruzic, D.E. Voss, and co-workers (1984). Nucl. Fusion 24, pp.1490-1494.
Cohen, S.A. (1984). In D.E. Post and R. Behrisch (Ed.), Physics of Plasma-Wall Interactions in Controlled Fusion, Plenum Press, New York. pp.773-854.
Cohen, S.A., J. Ehrenberg, D.V. Bartlett, and co-workers (1987). Proceedings 13th European Conference on Controlled Fusion and Plasma Physics, Madrid, Vol.11D, Part II. pp.694-697.
Dietz, J. and co-workers (1987). Private communication.
de Kock, L. and the JET Team (1987). J. Nucl. Mater., 145-147, pp.26-40.
Dylla, H.F. (1980). J. Nucl. Mater., 93 & 94, pp.61-70.
Dylla, H.F., P.H. LaMarche, M. Ulrickson, and co-workers (1987). Nucl. Fusion, in press.
Eckstein, W. and D. Heifetz (1987). J. Nucl. Mater., 145-147, pp.332-338.
Ehrenberg, J. (1987). J. Nucl. Mater., 145-147, pp.551-555.
Ehrenberg, J., S.A. Cohen, L. de Kock, and co-workers (1987). Proceedings 13th European Conference on Controlled Fusion and Plasma Physics, Madrid, Vol.11D, Part II. pp.706-709.
Engelhardt, W. and W. Feneberg (1978). J. Nucl. Mater., 76-77, pp.518-520.
Erents, S.K., J.A. Tagle, G.M. McCracken, and co-workers (1987). Proceedings 13th European Conference on Controlled Fusion and Plasma Physics, Madrid, Vol.11D, Part II. pp.740-743.
Eubank, H.P., R.J. Goldston, V. Arunasalam, and co-workers (1979). Phys. Rev. Lett. 43, 270-274.
Goebel, D.M., Y. Hirooka, R.W. Conn, and co-workers (1987). J. Nucl. Mater., pp.61-70.
Gondhalekar, A., M. Bures, D. Campbell, and co-workers (1987). In Plasma Physics and Controlled Fusion Research, IAEA, Vienna. IAEA-CN-47/I-I-6.
Greenwald, M., D. Gwinn, S. Milora and co-workers (1984). Phys. Rev. Lett., 53 p.352.
Hawryluk, R.J., V. Arunasalam, M.G. Bell, and co-workers (1987). Plasma Physics and Controlled Nuclear Fusion Research, IAEA, Vienna. IAEA-CN-47/A-1-3.
Hsu, W. and R. Causey (1987). J. Vac. Sci. and Technol. A5 (6). In press.
Hubbard, A., D. Ward and T.E. Stringer (1986). Proceedings 12th European Conference on Controlled Fusion and Plasma Physics, Schliersee, Part I. pp.232-235.
Jones, T.T.C., E. Thompson, A. Gondhalekar, and co-workers (1987). Proceedings 13th European Conference on Controlled Fusion and Plasma Physics, Madrid, Vol.11D, Part I. pp.17-19.
LaMarche, P., H.F. Dylla, P.J. McCarthy, and co-workers (1986). J. Vac. Sci. and Technol. A4, pp.1198-1202.
Lackner, K., R. Chodura, and M. Kaufmann (1984). Plasma Physics & Controlled Fusion, 26, 105-115.
McCracken, G.M. (1987). Plasma Physics & Controlled Fusion. This volume.
Mioduszewski, P. (1984). In D.E. Post and R. Behrisch (Ed.), Physics of Plasma-Wall Interactions in Controlled Fusion, Plenum Press, New York. pp.891-930.
Nakamura, H., T. Ando, S. Niikura, and co-workers (1986). JAERI-M 86-173.
Nakamura, K., S. Fukuda, T. Hino, and co-workers (1987). J. Nucl. Mater., 145-147, 301-304.
Philipps, V., E. Vietzke, M. Erdweg, and co-workers (1987). J. Nucl. Mater., 145-147, 292-296.
Rebut, P.H. and P.P. Lallia (1987). JET Preprint-P(87)15.
Rebut, P.H., M. Watkins and P. Lallia (1987). Proceedings 13th European Conference on Controlled Fusion and Plasma Physics, Madrid, Vol.11D, Part I. pp.172-175.
Roth, J. (1987). J. Nucl. Mater., 145-147, pp.87-95.
Scherzer, B.M.U., P. Borgesen and W. Möller (1987). IPP-JET-Report No.32.
Stangeby, P.C. (1987). J. Nucl. Mater., 145-147, pp.105-117.
Stangeby, P.C., J.A. Tagle, S.K. Erents and co-workers (1987). Proceedings 13th European Conference on Controlled Fusion and Plasma Physics, Madrid, Vol.11D, pp.670-673.
Staudenmaier, G., J. Roth, R. Behrisch, and co-workers (1979). J. Nucl. Mater. 84, 149.
Tagle, J.A., S.K. Erents, G.M. McCracken, and co-workers (1987). Proceedings 13th European Conference on Controlled Fusion and Plasma Physics, Madrid, Vol.11D, Part II. pp.662-665.
Voss, D.E. (1980). Ph.D. Thesis, Princeton University.
Wagner, F., M. Keilhacker and the ASDEX and NI Teams (1984). J. Nucl. Mater., 121, 103.
Wagner, F. and K. Lackner (1984). In D.E. Post and R. Behrisch (Ed.), Physics of Plasma-Wall Interactions in Controlled Fusion, Plenum Press, New York. pp.931-1004.
Wampler, B. and B. Doyle (1987). Private communication.
Wang, Y.G., W.P. Poschenrieder and G. Venus (1986). J. Vac. Sci. and Technol. A4, pp.2520-2525.
Wilson, K. and Hsu, W. (1987). J. Nucl. Mater., 145-147, pp.121-130.
Winter, J. (1987a). J. Nucl. Mater., 145-147, pp.131-145.
Winter, J. (1987b). J. Vac. Sci. and Technol., A5(6). In press.